# Protein Engineering Using Molecular Assembly: Functional Conversion of Cytochrome *c* via Noncovalent Interactions

**Itaru Hamachi,* Akio Fujita, and Toyoki Kunitake***

*Contribution from the Department of Chemistry & Biochemistry (Molecular Science Engineering), Kyushu University, Hakozaki, Fukuoka 812-81, Japan*

*Received April 14, 1997*[⊗]

**Abstract:** The structure−function relationship of cytochrome *c* (Cyt-*c*) interacted with the lipid bilayer membranes was studied by various spectroscopic methods, the reaction−products analysis, and its kinetics. Ultrafiltration binding assay, UV−visible, electron paramagnetic resonance (EPR), and circular dichroism (CD) spectroscopies showed that Cyt-*c* was tightly bound to the lipid bilayer membranes bearing a phosphate head group. The anisotropic and nonnatural complexation with the phosphate−lipid membranes caused a spin-state change of the heme in the active center of Cyt-*c*. Depending on the membrane fluidity, two classes of the structurally altered Cyt-*c* were prepared and they showed the greatly enhanced *N*-demethylase activity. Products analysis by HPLC demonstrated that the lipid membrane bound Cyt-*c* performs a clean enzymatic reaction similar to native hemoenzymes. Kinetics studies established that there are two different activation manners via the phosphate lipid bilayer membranes: namely, simple enhancement of the affinity for $H_2O_2$, or the increased catalytic efficiency ($k_{cat}$) in addition to the enhanced affinity for $H_2O_2$. The membrane fluidity again significantly affected the N-demethylation kinetics. A potential of the lipid membrane assembly to functionalize native proteins and enzymes with noncovalent but specific interactions is also discussed.

## Introduction

Hybridization of naturally occurring enzymes and proteins with artificial molecules is one of the most promising methods for the development of protein-based biomaterials. Among the diverse artificial molecules, employment of self-organized molecular assemblies is regarded as a unique approach. The potential application for biosensors of enzyme−electrode composites that use a self-assembled monolayer or multilayer films has led to vigorous investigation of these artificial molecules.[1] Enzymes encapsulated in reversed micelles or polymer aggregates are applied as useful biocatalysts in some organic synthetic (enantio- or regioselective) reactions, as well as the separation processes of native enzymes.[2] Protein−hydrophobic polysaccharide aggregates have been proposed as a supramolecular drug delivery system.[3]

In order to expand the potential of the molecular self-assembly to functionalize native proteins as novel materials, how self-assemblies affect the structure and activity of native enzymes/proteins in basic molecular terms must be clarified. Because the interactions between biopolymers and the molecular assemblies are so complicated, a suitable model system is required. In a pioneering approach, a series of the recent resonance Raman experiments by Hildebrandt and co-workers resulted in a unique conformational change of cytochrome *c* (Cyt-*c*), an electron-transporting hemoprotein, upon electrostatic binding to charged interfaces such as phospholipid vesicles, a reversed micelle, and heteropolytungstates.[4] With respect to the intrinsic reactivity of Cyt-*c*, during our study of the functional conversion of hemoproteins by synthetic lipid bilayer assemblies, we identified the enhanced peroxidase and *N*-demethylase activities of Cyt-*c* bound to a lipid bilayer membrane.[5]

In the present article, we provide additional data on the *N*-demethylase activity of Cyt-*c* induced by synthetic lipid bilayer membranes bearing a phosphate head group (phosphate lipid bilayer) and more importantly, discuss the relationship between the lipid membranes-induced activity of Cyt-*c* and the structural changes. We propose a method for noncovalent but efficient protein engineering with supramolecular self-assembly systems.

## Results

In order to investigate the structure and activity changes of Cyt-*c* induced by lipid bilayer membranes, we used a variety of synthetic lipids as shown in Chart 1.

**Affinity of Cyt-*c* for Various Synthetic Lipid Bilayer Membranes.** Binding of Cyt-*c* to various lipid bilayer mem-

* Author to whom correspondence should be addressed. E-mail: itarutcmcmbox.nc.kyushu-u.ac.jp.

⊗ Abstract published in *Advance ACS Abstracts,* September 15, 1997.

(1) (a) Turner, A. P. F., Karube, M., Wilson, G. S., Eds. *Biosensors: Fundamentals and Applications*; Oxford University Press: Oxford, 1987. (b) Yasuda, Y.; Sugino, H.; Toyotama, H.; Hirata, Y.; Hara, M.; Miyake, J. *Bioelectrochem. Bioenerg.* **1994**, *36*, 135. (c) Cullison, J. K.; Hawkridge, F. M.; Nakashima, N.; Yoshikawa, S. *Langmuir* **1994**, *10*, 877. (d) Rusling, J.; Nassar, A. E. F. *J. Am. Chem. Soc.* **1993**, 115, 11891. (f) Nassar, A. E. F.; Bobbitt, J. M.; Stuart, J. D.; Rusling, J. *J. Am. Chem. Soc.* **1995**, *117*, 10986. (g) Ulman, A. *An Introsuction to Ultrathin Organic Films: from L-B to Self-Assembly*; Academic Press: San Diego, 1991. (h) Katz, E.; Schlereth, D. D.; Sxhmidt, H. L.; Olsthoorn, A. J. J. *J. Electroanal. Chem.* **1994**, *368*, 165.

(2) (a) Shield, J. W.; Ferguson, H. D.; Bommarius, A. S.; Hatton, T. A. *Ind. Eng. Chem. Fundam.* **1986**, *25*, 603. (b) Mosbach, K. *Methods Enzymol.* **1988**, *137*, 583. (c) Klibanov, A. M. *Anal. Biochem.* **1979**, *93*, 1. (d) Naka, K,; Kubo, Y.; Ohki, A.; Maeda, S. *Polym. J.* **1994**, *26*, 243.

(3) (a) Nishikawa, T.; Akiyoshi, K.; Sunamoto, J. *Macromolecules* **1994**, *27*, 7654. (b) Akiyoshi, K.; Nishikawa, T.; Shichibe, S.; Sunamoto, J. *Chem. Lett.* **1995**, 707. (c) Akiyoshi, K.; Nagai, K.; Nishikawa, T.; Sunamoto, J. *Chem. Lett.* **1995**, 1727. (d) Nishikawa, T.; Akiyoshi, K.; Sunamoto, J. *J. Am. Chem. Soc.* **1996**, *118*, 6110.

(4) (a) Hildebrandt, P.; Stockburger, M. *Biochemistry* **1989**, *28*, 6710. (b) Hildebrandt, P.; Stockburger, M. *Biochemistry* **1989**, *28*, 6722. (c) Hildebrandt, P.; Heimburg, T.; Marsh, D. *Eur. Biophys. J.* **1990**, *18*, 193. (d) Heimburg, T.; Hildebrandt, P.; Marsh, P. *Biochemistry* **1991**, *30*, 9084. (e) Muga, A.; Mantsch, H. H.; Surewicz, W. K. *Biochemistry* **1991**, *30*, 7219. (f) Hildebrandt, P. In *Cytochrome c-A multidisciplinary approach*; Scott. R. A., Mauk, A. G., Eds.; University Science Book: Sausalito, CA, 1996; p 285.

(5) (a) Hamachi, I.; Fujita, A.; Kunitake, T. *J. Am. Chem. Soc.* **1994**, *116*, 8811. (b) Fujita, A.; Senzu, H.; Kunitake, T.; Hamachi, I. *Chem. Lett.* **1994**, 1219.

S0002-7863(97)01177-3 CCC: $14.00 

**Chart 1**

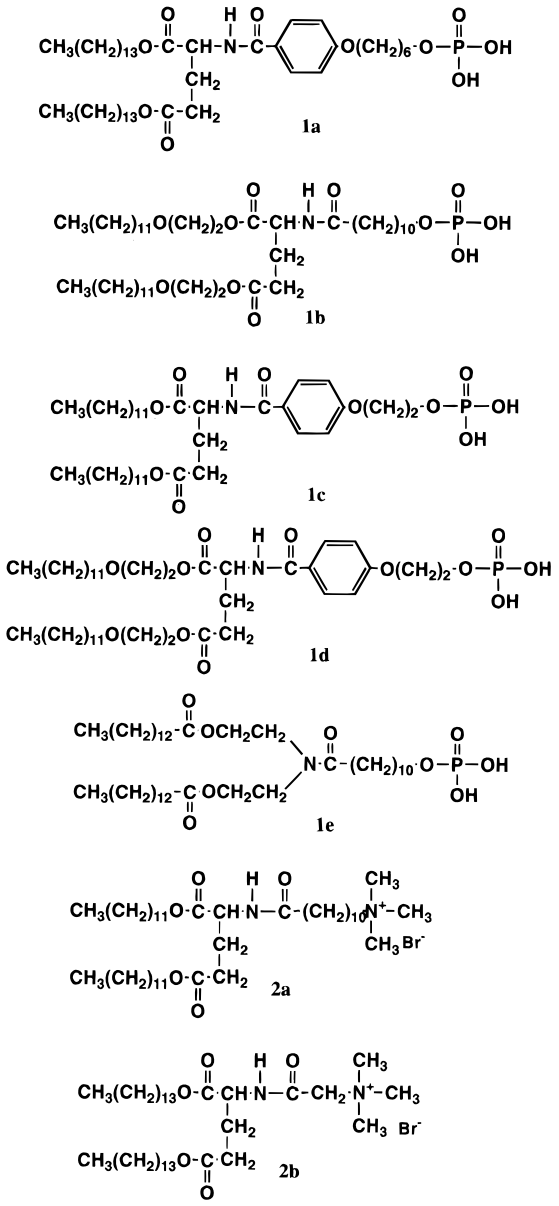


branes was evaluated using the ultrafiltration binding assay.[6] The fraction of Cyt-*c* bound to the phosphate lipid bilayer **1a, 1b, 1c**, and **1d,** an ammonium−lipid bilayer, **2a,** and a zwitterionic DMPC **3,** was 96, 98, 90, 95, 6, and 10%, respectively. Clearly, the *N*-demethylase bilayers tightly bound Cyt-*c* under neutral pH, because of the high isoelectric point of Cyt-*c* (p$I$ = 10).[7] Next, the binding of Cyt-*c* with a mixed lipid bilayer membrane of **1a** and DMPC **3** was evaluated. When the lipid bilayer membrane consisted of less than 10% **1a**, only 10% Cyt-*c* bound. As the percentage of **1a** in the mixed lipid bilayer membrane increased, the amount of membrane-bound Cyt-*c* sigmoidally increased (shown in Figure 1).[8] These results indicate that Cyt-*c* is selectively bound to an anionic phosphate lipid bilayer membrane.

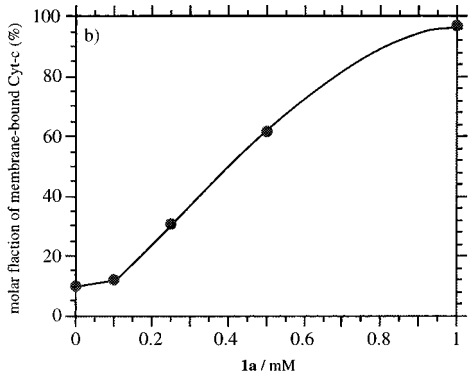


**Figure 1.** Binding assay of Cyt-*c* with the mixed lipid bilayer membrane comprising of the phosphate−lipid **1a** and DMPC **3**: Cyt-*c* 5 $\mu$M, **1a** + **3** = 1mM, in 25 mM phosphate buffer (pH 7.0).

**Lipid Bilayer-Induced Structural Changes in Cyt-*c*.** Structural changes in Cyt-*c* bound to the lipid bilayer membranes were examined using UV−visible absorption, electron paramagnetic resonance (EPR), and circular dichroism (CD) spectroscopy. Table 1 compares the UV−visible spectrum of native Cyt-*c* with those of the membrane-bound Cyt-*c* both in the oxidized (Fe(III)) and reduced (Fe(II)) forms. A sharp Soret band at 408 nm, a broad Q band at 560 nm and a very weak charge-transfer (LMCT) band from the sulfur atom of Met 80 (the axial ligand) to heme iron(III) at 695 nm are observed for the oxidized form of native Cyt-*c*.[9] Slight shift of the Soret band (406 nm) and complete disappearance of the LMCT band are apparent in the spectrum of **1a**-bound Cyt-*c*. The Soret band shows a distinct red shift (from 416 to 426 nm) with smaller extinction coefficient ($\epsilon$ = 85 mM$^{-1}$ cm$^{-1}$) for the reduced form of **1a**-bound Cyt-*c*.[10] Two characteristic Q bands of native Cyt-*c* at 550 and 520 nm became one broad band (550 nm) in the **1a**-bound Cyt-*c* spectrum. These spectral changes reveal the complete cleavage of the coordination bond of Met 80 to iron(III) upon binding to the phosphate lipid bilayer membrane **1a**.

On the other hand, **1d**-bound Cyt-*c* displays different spectral behavior. For the oxidized state, in the **1d**-bound Cyt-*c* spectrum, although the LMCT band remained at 70% of the native Cyt-*c* intensity, the other peaks closely resembled those obtained for the case of **1a**-bound Cyt-*c*. Two Q bands (550 and 520 nm) and a sharp Soret band (415 nm) similar to the native bands were clearly retained in the reduced form. These spectral characteristics suggest that **1d**-bound Cyt-*c* exists in equilibrium between a high-spin (i.e., broken Met−80 iron bond) and a low-spin (i.e., coordinated Met 80−iron bond) state. The 1:2 ratio (the high-spin species:the low-spin species) is roughly estimated from the intensity of LMCT band. No changes occur upon addition of ammonium lipid **2a** or zwitterionic **3**.

The spin-state alteration of the active site of Cyt-*c* was directly monitored using EPR at 20 K. Figure 2 shows the EPR spectra of frozen solutions in the presence and absence of the lipid bilayer membranes. Without lipid membranes, two peaks at $g$ = 3.0 and 2.3 appear as reported in the literature, indicating a ferric low-spin state (Figure 2a).[11] The signals due to the low spin are remarkably reduced for the **1a**-bound Cyt-*c* (Figure 2b). Instead, a strong peak ($g$ = 5.9) and a weak peak ($g$ =

(6) (a) Hamachi, I.; Nakamura, K.; Fujita, A.; Kunitake, T. *J. Am. Chem. Soc.* **1993**, 115, 4966. (b) Hamachi, I.; Higuchi, S.; Nakamura, K.; Fujimura, H.; Kunitake, T. *Chem. Lett.* **1994**, 1219.

(7) Barlow, G. H.; Margoliash, E. J. *J. Biol. Chem.* **1966**, *241*, 1473.

(8) In the mixed lipid membrane of the lower content of **1a** (less than 10 %), it is reasonable to consider that **1a** is homogeneously dispersed in the DMPC lipid. With increase of the **1a** ratio, the lipid **1a** easily aggregates to form a cluster in the mixed membrane. The sigmoidal curve for the binding affinity study suggests that such a cluster structure of **1a** is needed for the Cyt-*c* binding. The *N*-demethylase activity was also found to be sigmoidal in the presence of the mixed lipid bilayer membrane.

(9) (a) Sreenathan, B. R.; Taylor, C. P. S. *Biochem. Biophys. Res. Commun.* **1971**, *42*, 1122. (b) Schechter, E.; Saludjian, P. *Biopolymers* **1967**, *5*, 788. (c) Kaminsky, L. S.; Ivanetich, K. M.; King, T. E. *Biochemistry* **1974**, *13*, 4866.

(10) The molecular extinction coefficient of native Cyt-*c* (reduced form) was reported to be 129.1 /mM cm. Margoliash, E.; Frohwirt, N. *J. Biochem.* **1959**, *71*, 570.

(11) Ikeda-Saito, M.; Iizuka, T. *Biochim. Biophys. Acta* **1975**, *393*, 335.

**Table 1.** Absorption Spectra of Cyt-*c* Derivatives

| | ferric state ($\lambda_{max}$ ($\epsilon_{mM}$)) | | | ferrous state ($\lambda_{max}$ ($\epsilon_{mM}$)) | | |
|---|---|---|---|---|---|---|
| | | | | Q band, nm | | |
| hemoprotein | S→Fe charge transfer (695 nm) | Q band ($\alpha/\beta$), nm | Soret band, nm | $\alpha$ | $\beta$ | Soret band, nm |
| native Cyt-*c* | yes | 528 | 409 (106.1) | 550 (29.5) | 520 | 415 (129.1) |
| bilayer **1a**-bound Cyt-*c* | no | 525 | 406 | | 550 (broad; 11.6) | 426 (98) |
| bilayer **1b**-bound Cyt-*c* | no | 523 | 407 | | 550 (broad; 14.5) | 418 (102.5) |
| bilayer **1c**-bound Cyt-*c* | no | 530 | 407 | | 550 (broad; 12.9) | 419 (91) |
| bilayer **1d**-bound Cyt-*c* | yes[a] | 525 | 407 | 550 (19.7) | 520 | 415 (107) |
| bilayer **1e**-bound Cyt-*c* | no | 528 | 407 | | 550 (broad; 10.3) | 428 (88) |
| myoglobin | | 502 | 409 | | 556 (broad) | 434 |

[a] Mixture of high-spin and low-spin states.

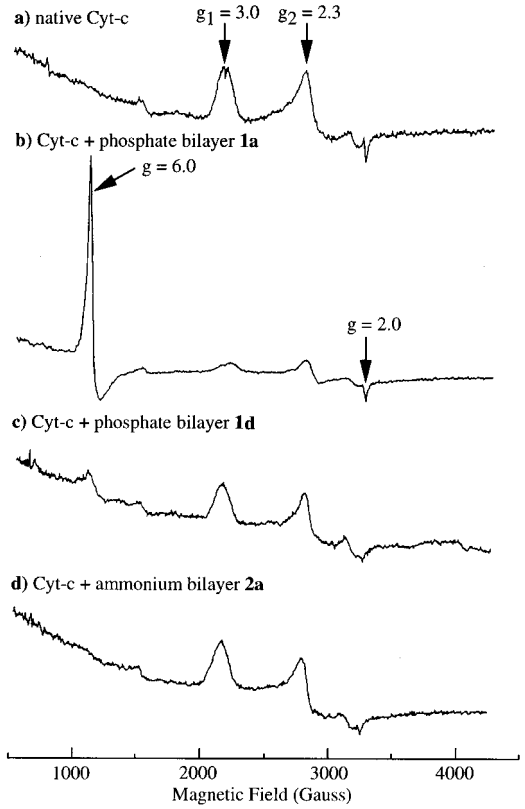


**Figure 2.** EPR spectra of frozen solutions containing Cyt-*c* in the absence and presence of lipid bilayer membranes at 20 K: Cyt-*c* 210 $\mu$M, 8.3 mM of lipid 10 mM of the phosphate buffer (pH 7.0). (a) without lipid, (b) with **1a**, (c) with **1d**, (d) with **2a**. EPR conditions: in a quartz EPR tube (diameter 2 mm), JEOL JES-2X X-band EPR spectrophotometer equipped with a microwave liquid helium cryostat with 100 kHz magnetic field modulation, 5 mW microwave power, 0.79 mT modulation amp.

2.0) which are ascribed to the ferric high-spin state emerge.[12] In sharp contrast, the EPR spectrum of **1d**-bound Cyt-*c* is almost identical to the ferric low-spin state (Figure 2c) and the high-spin component is not observed at 20 K.[13] EPR signals of Cyt-*c* in the presence of ammonium **2a** (Figure 2d) and zwitterionic **3** (data not shown) lipid bilayers do not differ from those of native Cyt-*c*.

Figure 3 shows the CD spectra of Cyt-*c* in the presence of various phosphate−lipid bilayer membranes. A negative (419 nm) and a positive (410 nm) peak due to a split Cotton effect are observed for native Cyt-*c* (represented as - - - in Figure 3).[14]

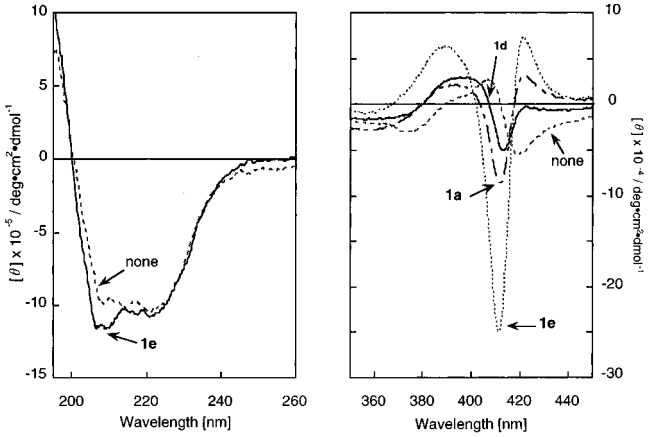


**Figure 3.** CD spectra of the *N*-demethylase bilayer membranes-bound Cyt-*c*: (a) Soret band region and (b) the amide bond region.

When Cyt-*c* is bound to **1a** (− · −, Cyt-*c*/**1a**), the CD spectrum changes markedly and exhibits a positive (423 nm) peak, a strong negative (412 nm) peak, and a weak positive (393 nm) peaks. A similar but intensified CD pattern is observed for Cyt-*c*/**1e** (···). In contrast, the CD spectrum of Cyt-*c*/**1d** is very different; the positive peak at 423 nm disappears, and instead a sharp negative (413 nm) band and a broad positive (398 nm) band are observed. Thus, the heme environment of **1d**-bound Cyt-*c* appears to be different from **1a**-bound Cyt-*c*. It should be noted that these spectra are distinct from that of urea-denatured Cyt-*c* in which a broad and less structured CD signal at 410nm (positive) is observed.[15] In addition, the CD spectrum of the $\alpha$-helix region for Cyt-*c*/**1e** is almost identical to that of native Cyt-*c*.[16] Clearly, the *N*-demethylase induced structural changes of Cyt-*c* are not due to a simple denaturation.

**Anisotropic Binding of Cyt-*c* to the Phosphate-Lipid Bilayer Membranes.** The molecular orientation of Cyt-*c* on the lipid bilayer membrane was examined using the angular dependence of EPR measurement of the immobilized lipid film containing Cyt-*c* at the temperature of liquid helium (4 K).[17] EPR spectra of the film of the Cyt-*c*/**1a** composite were measured at different angles ($\phi$) of the normal of the film plane against the direction of the applied magnetic field (Figure 4). The EPR signals appeared to change depending on the angle. When the film plane was disposed parallel to the magnetic field ($\phi = 90°$), an intense signal at $g = 5.9$ ($g_\perp$ component of the $g$ parameters) and a very weak signal at $g = 2.0$ ($g_\parallel$ component)

(12) The observed $g$ values and the signal pattern are closely similar to those of myoglobin which has His and $H_2O$ coordinated to the heme iron. Yonetani, T.; Schleyer, H. *J. Biol. Chem.* **1967**, *242*, 3926.

(13) For **1d**-bound Cyt-*c*, the low spin state became predominant at 20 K, instead of the spin-state equilibrium at room temperature.

(14) Myer, Y. P. *Methods Enzymol.* **1978**, *54*, 249.

(15) Myer, Y.P.; MacDonald, L. M.; Verma, B. C.; Pande, A. *Biochemistry* **1980**, *19*, 199.

(16) Unfortunately, a strong CD band due to the chiral amide residue of the lipids **1a** and **1d** prevented us from estimating the $\alpha$-helix region by CD spectroscopy.

(17) This technique has been utilized for determining the orientation of membrane-bound hemoproteins and iron−sulfur proteins in biomembranes. Blasie, J. K.; Erecinska, M.; Samuels, S.; Leigh, J. S. *Biochim. Biophys. Acta* **1978**, *501*, 33.

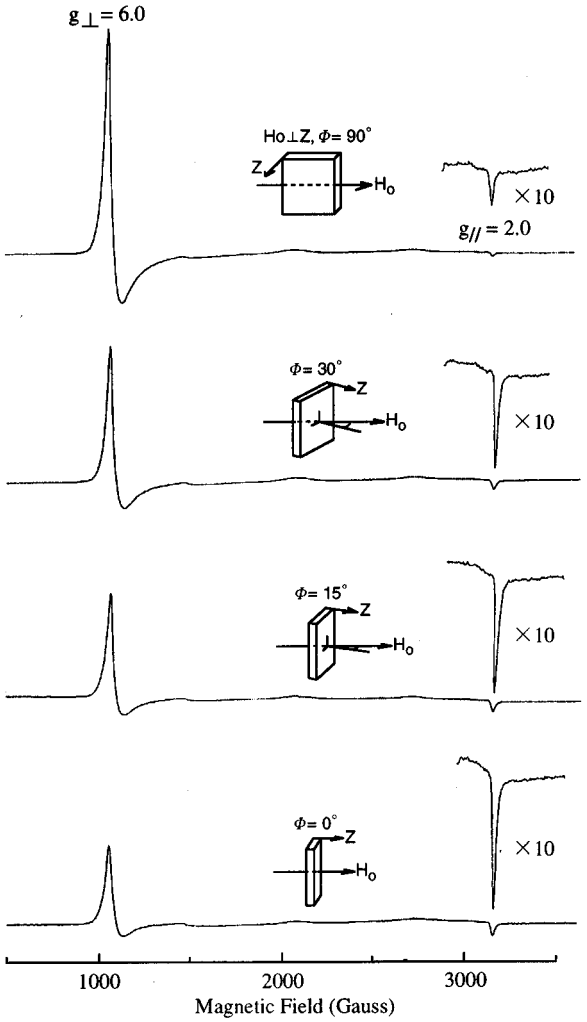


**Figure 4.** Angular dependence of EPR spectra of Cyt-*c* immobilized in a cast film of **1a**: Cyt-*c*/**1a** = 1/200 (mol/mol) at 5 K. EPR conditions are same as Figure 2.

were observed. As the angle decreases to 0°, the $g_\perp$ signal is weakened and $g_{||}$ is intensified. The present angular dependence of both *g* components implies that the heme plane in Cyt-*c* is oriented almost parallel relative to the lipid multilayer film plane (i.e., parallel to the lipid bilayer **1a** surface).[18] Similar orientation of Cyt-*c* has been reported in anionic Langmuir−Blodgett films and self-assembled monolayers on gold.[19] This orientation of Cyt-*c* has been ascribed to the electrostatic interaction between the cationic domain of Cyt-*c* and the anionic membrane surfaces. Notably, the present regular orientation indicates that the phosphate lipid bilayer **1a** anisotropically acts upon the specific domain of Cyt-*c*.[20]

**Lipid Bilayer-Enhanced *N*-Demethylase Activity of Cyt-*c*.** The above findings with respect to the structural changes in membrane-bound Cyt-*c* suggest that the axial site of the heme

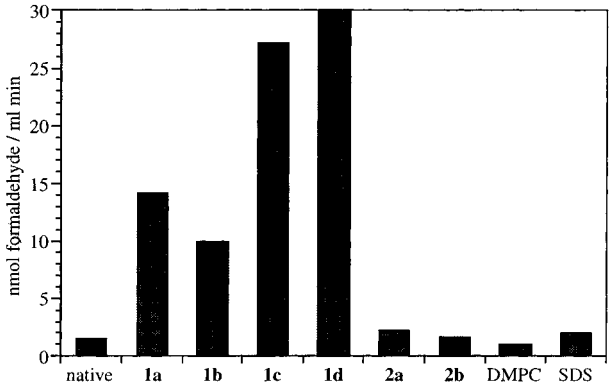


**Figure 5.** The initial rates of *N*-demethylase activity of Cyt-*c* in the absence and presence of various lipid bilayer membranes: Cyt-*c* 5 $\mu$M, NNDA 2 mM, $H_2O_2$ 1 mM, lipid 0.25 mM in 25 mM phosphate buffer (pH 7.0) at 30 °C.

is available to react with small molecules, just like the heme center of peroxidase or monooxygenase in the family of hemoenzymes. N-Demethylation is one of the typical oxidation reactions catalyzed by such hemoenzymes. Thus we evaluated the catalytic activity of Cyt-*c* in the presence of the various lipid bilayer membranes using a N-demethylation reaction of *N*,*N*-dimethylaniline (eq 1). The initial reaction rates were

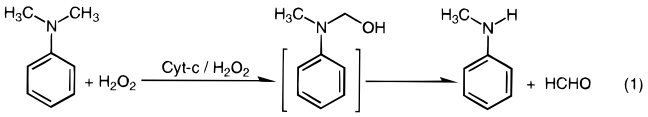


determined by detecting the amount of formaldehyde produced[21] and are summarized in Figure 5. The addition of **1a** accelerated the initial reaction rate (14 nmol/mL min) by 10-fold, relative to that of native Cyt-*c* (i.e., without lipid bilayers, the reaction rate is 1.3 nmol/(mL min)). This rate enhancement produced typical saturation behavior with respect to the **1a** concentration (data not shown). Other *N*-demethylase bilayer membranes also enhanced the reaction rate (11 nmol/(mL min) for **1b**, 27 nmol/(mL min) for **1c** and 30 nmol/(mL min) for **1d**). In contrast, the reaction rates in the presence of the ammonium−lipid bilayers were almost identical to that of native Cyt-*c* (2.0 nmol/(mL min) for **2a** and 1.6 nmol/(mL min) for **2b**). The reaction was moderately suppressed by the addition of zwitterionic lipid **3** (0.8 nmol/(mL min)). An anionic micelle, sodium dodecyl sulfate (SDS), did not influence the rate (2.0 nmol/(mL min)). These results suggest that the phosphate−lipid bilayer membranes enhance the *N*-demethylase activity of Cyt-*c*.

**Analysis of the *N*-Demethylation Reaction.** Figure 6a shows a HPLC (high-performance liquid chromatography) chart obtained during the demethylation reaction catalyzed by the **1a**-bound Cyt-*c*. We observed only two peaks; the peak due to the starting material (*N*,*N*-dimethylaniline (NNDA), retention time $t_R$ = 5.4 min) and the product (*N*-methylaniline, $t_R$ = 3.8 min) in addition to the peaks of the solvent (trichloroacetic acid) and the internal standard (*N*-ethylaniline). No other peaks due to byproducts were detected, indicating that the present demethylation is a clean oxidation reaction with no considerable side reactions. Figure 6b displays the time courses of *N*-methylaniline and formaldehyde produced, along with that of the consumed $H_2O_2$. The amount of *N*-methylaniline produced as determined by HPLC is in good agreement with that of formaldehyde produced as determined by the Nash method. The stoichiometry of consumed $H_2O_2$ to product is 2:1. This ratio is different from the native peroxidase-catalyzed *N*-demeth-

(18) The direction of $\mathbf{g}_{||}$ tensor is assigned parallel to the normal axis of the heme plane and the direction of $g_\perp$ components are in the heme plane. The *g* signal is intensified when the direction of **g** tensor is parallel to the direction of the applied magnetic field. The simulation was conducted according to the same manner reported by us. (a) Hamachi, I.; Noda, S.; Kunitake, T. *J. Am. Chem. Soc.* **1991**, *113*, 9625. (b) Ishikawa, Y.; Kunitake, T. *J. Am. Chem. Soc.* **1991**, *113*, 621.

(19) (a) Pachence, J. M.; Blasie, J. K. *Biophys. J.* **1987**, *52*, 735. (b) Pachence, J. M.; Fischetti, R. F.; Blasie, J. K. *Biophys. J.* **1989**, *56*, 327. (c) Pachence, J. M.; Amador. S. M.; Mamoara, G.; Vanderkooi, J.; Dutton, P. L.; Blasie, J. K. *Biophys. J.* **1990**, *58*, 379.

(20) Since the phosphate lipid **1d** did not form a stable cast film, we could not evaluate the orientation of Cyt-*c* against the membrane comprising of **1d**.

(21) Werringloer, J. *Methods Enzymol.* **1978**, *52*, 297.

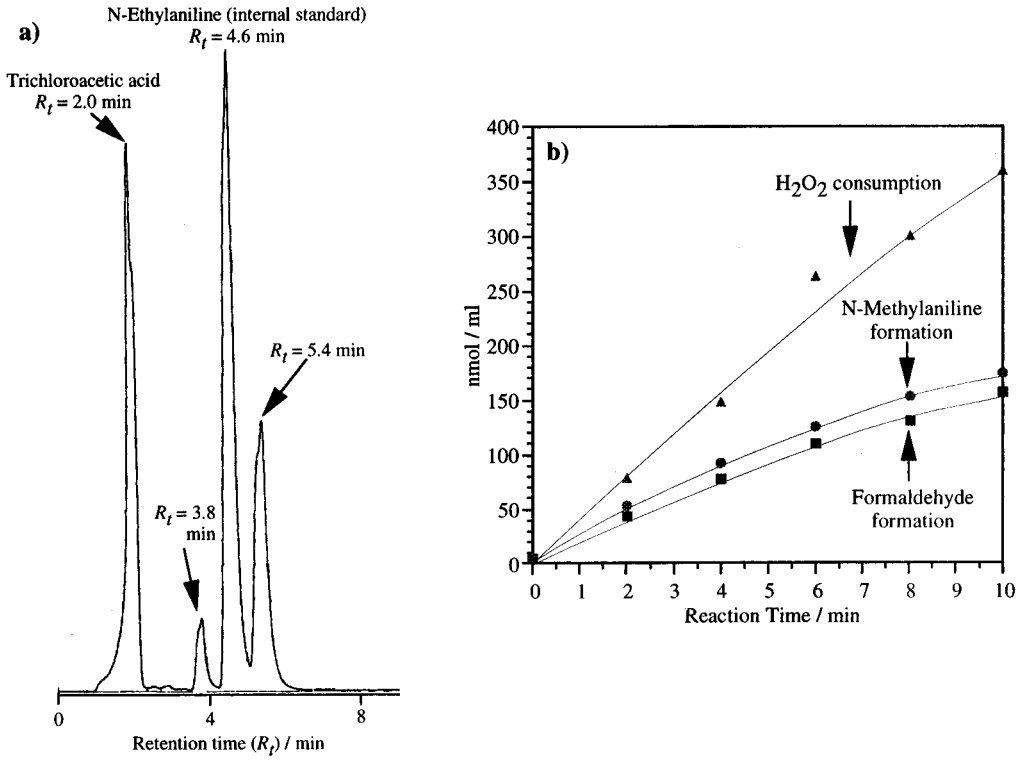


**Figure 6.** Assay of the products formed during the N-demethylation reaction catalyzed by **1a**-bound Cyt-*c*: (a) HPLC elution profile of the reaction mixture at the reaction time of 6 min and (b) time courses of the amounts of the produced formaldehyde and *N*-methylaniline, and of the consumed $H_2O_2$.

ylation (stoichiometry of 1:1).[22] Therefore, the oxidation efficiency (the ratio of the product based on the oxidant; i.e., [product]/ [$H_2O_2$]) is 0.5 for the present system and 1 for the native peroxidase system. This reduction in efficiency suggests that the present reaction system contains some nonproductive side reactions that waste $H_2O_2$.[23] Similar behavior was observed for the other *N*-demethylase bilayer bound Cyt-*c* samples.

The hemoenzyme-catalyzed N-demethylation has been reported to proceed via two major steps, in which the hemoenzyme reacts with $H_2O_2$ to form an active intermediate (a hypervalent iron-oxo species was confirmed in some cases), followed by the oxidation of substrates (NNDA in this case).[24] All attempts to detect the active intermediates of Cyt-*c* failed in our system due to the instability. Instead, rapid decomposition of the heme unit of Cyt-*c* occurred in the absence of NNDA and the decomposition rate was simply suppressed by the addition of NNDA. The heme degradation rate in the absence of NNDA was dependent on the type of lipid bilayer membrane. In the presence of **1a**, the initial rate (2.5 $\mu$M/min) was greatly accelerated, relative to that in the absence of lipids (0.27 $\mu$M/min), or relative to **2a** (0.26 $\mu$M/min) or to **3** (0.25 $\mu$M/min). Interestingly, the rate in the presence of **1d** (11.0 $\mu$M/min) was 4 times greater than that of **1a**.[25]

The autooxidation rate of the reduced Cyt-*c* was also accelerated by the addition of the phosphate lipid bilayers as shown in Figure 7. The reduced Cyt-*c* without lipids was hardly autooxidized under aerobic conditions (less than 0.01 $\mu$M/min) because of the tightly coordinated axial ligands of His 18 and Met 80.[26] The fast autooxidation (1.6 $\mu$M/min) of Cyt-*c* occurred upon binding to **1a**. Binding to phosphate lipid **1d** (4.4 $\mu$M/min) was again more effective than **1a**. Conceivably, **1a**-bound Cyt-*c* or **1d**-bound Cyt-*c* acquired *N*-demethylase activity, instead of losing native electron-transfer activity under aerobic conditions. The ammonium lipid **2a** and DMPC **3** did not facilitate the autooxidation reaction.

**Kinetics of N-Demethylase Activity of Membrane-Bound Cyt-*c*.** The hemoprotein-catalyzed N-demethylation by $H_2O_2$ is regarded as a typical two-substrate reaction in general. The initial rate was found not to be sensitive to the concentration of NNDA, but dependent on the concentration of $H_2O_2$ in a saturation manner. Therefore, the rate-determining step of the overall reaction was assigned to the generation step of the active intermediate of Cyt-*c* with $H_2O_2$. Under these conditions, double-reciprocal plots of the initial rates against the $H_2O_2$ concentration yielded satisfactorily linear relationships as shown in Figure 8. The parameters obtained in the Michaelis−Menten scheme were as follows: $k_{cat}$ = 9 min$^{-1}$, $K_m$ = 2 mM in the presence of **1a**, $k_{cat}$ = 87 min$^{-1}$, $K_m$ = 5 mM in the presence of **1d**-bound Cyt-*c*, $k_{cat}$ = 10 min$^{-1}$, $K_m$ = 28 mM in the presence of Cyt-*c* with **2a**, and $k_{cat}$ = 12 min$^{-1}$, $K_m$ = 40 mM for Cyt-*c* without lipids. The following points should be noted: (i) $K_m$ for the phosphate−lipids **1a** and **1d** are greatly lower than the value in the absence of lipids; (ii) the $k_{cat}$ value for **1a** is almost identical with that in the absence of lipids, whereas $k_{cat}$ for **1d** is 7-fold greater; (iii) the kinetic parameters for **2a** are the same as those in the absence of lipids within the margin of experimental errors. These results indicate that phosphate lipid **1a** facilitates the *N*-demethylase activity of Cyt-*c* by the increased affinity of Cyt-*c* for $H_2O_2$ ($1/K_m$), not by the catalytic efficiency ($k_{cat}$). In contrast, in the case of **1d**, the enhanced net activity is reasonably ascribed to not only the increased

(22) Kedderis, G. L.; Hollenberg, P. F. *J. Biol. Chem.* **1983**, *258*, 8129.
(23) The catalase-like reaction ($2H_2O_2 \rightarrow 2H_2O + O_2$) might be a candidate of such a reaction. We actually confirmed that $H_2O_2$ was consumed by **1a**-bound Cyt-*c* in the absence of NNDA.
(24) (a) Kedderis, G. L.; Koop, D. R.; Hollenberg, P. F. *J. Biol. Chem.* **1980**, *255*, 10174. (b) Kedderis, G. L.; Hollenberg, P. F. *J. Biol. Chem.* **1983**, *258*, 12413. (c) Miwa, G. T.; Walsh, J. S.; Kedderis, G.L.; Hollenberg, P. F. *J. Biol. Chem.* **1983**, *258*, 14445.
(25) The order of the magnitude of the heme-degradation rate was in good correspondence with that of the net *N*-demethylase activity.
(26) Bushnell, G. W.; Louie, G. V.; Brayer, G. D. *J. Mol. Biol.* **1983**, *214*, 585.

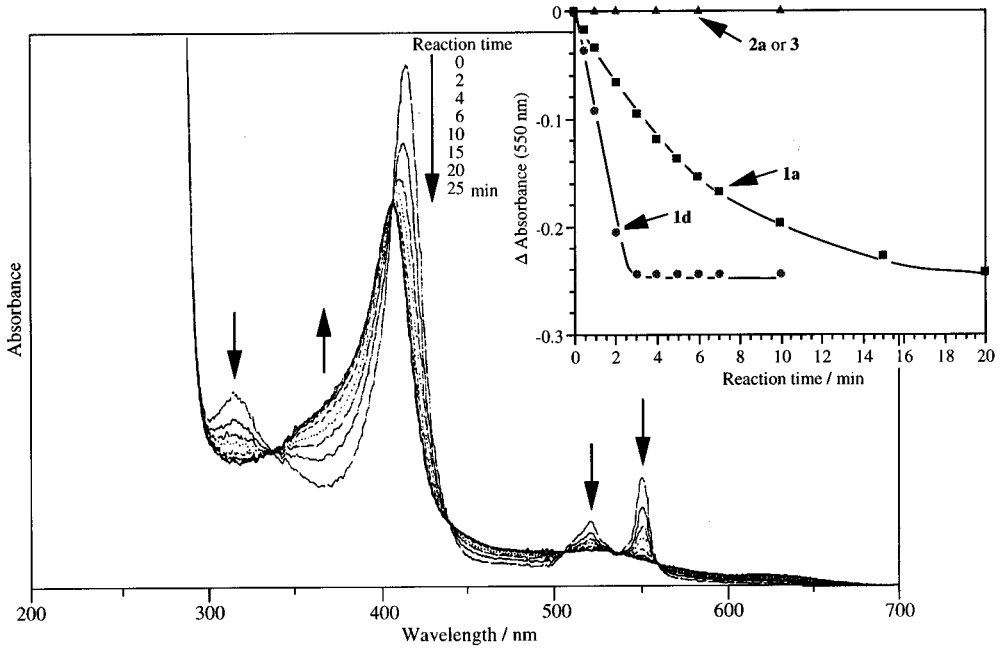


**Figure 7.** UV−visible spectral change of the autooxidation process of the reduced Cyt-*c* by addition of **1a**. (Inset) Time course of autooxidation of the reduced Cyt-*c* in the presence of various lipid bilayer membranes: 10 $\mu$M of Cyt-*c* in 10 mM phosphate buffer (pH 7.0) under aerobic conditions. The reaction was initiated by the addition of the lipid bilayer dispersion.

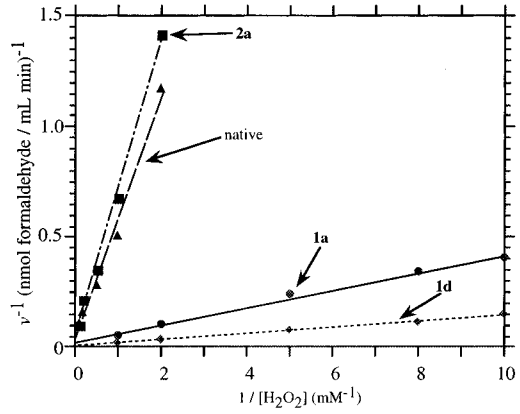


**Figure 8.** Double-reciprocal (Lineweaver−Burk) plots of the initial rate of *N*-demethylation by Cyt-*c* against $H_2O_2$ concentration in the absence and presence of the lipid bilayer membranes (**1a, 1d, 2a**): Cyt-*c* 5 $\mu$M, NNDA 2 mM, lipid 1 mM, in the phosphate buffer(pH 7.0).

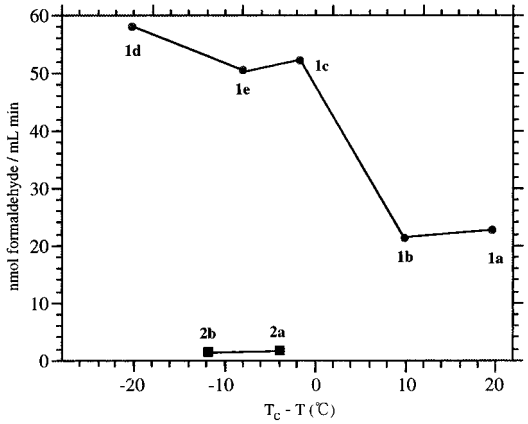


**Figure 9.** Dependence of the initial rates of N-demethylation reaction catalyzed by Cyt-*c* in the presence of the lipid membranes on $T_c$ (phase transition temperature): $T_c - T$, the difference between the phase transition temperature of the corresponding lipid membranes and the reaction temperature (38 °C).

affinity for $H_2O_2$, but also the enhanced catalytic efficiency of the membrane-bound Cyt-*c*.

## Discussion

Two classes of structurally altered Cyt-*c* were prepared upon binding to different phosphate lipid bilayer membranes; Cyt-*c* bearing the high spin state of heme (**1a**-bound Cyt-*c*) or Cyt-*c* bearing the heme in an equilibrium between the high spin and the low spin state (**1d**-bound Cyt-*c*). This is consistent with the results obtained by Hildebrandt and co workers.[4] Cyt-*c* is known to possess cationic lysine clusters.[26,27] When Cyt-*c* interacts with cyt-*c*-oxidase (CcO), a natural electron-accepting partner, the lysine cluster surrounding the heme crevice of Cyt-*c* binds to the negatively charged domain of CcO. If the same lysine cluster is employed to attach Cyt-*c* to the phosphate−lipid membrane, the heme of Cyt-*c* can be assumed to be oriented perpendicular to the membrane surface. However, the heme orientation has been determined to be parallel to the membrane surface. This implies that another cationic domain which is not used in the natural system interacts with the membrane surface. Such a nonnatural electrostatic interaction may play a crucial role in the structural perturbation of the membrane-bound Cyt-*c*.

Interestingly in the present study, these structurally perturbed Cyt-*c* molecule showed enhanced *N*-demethylase activity. Product analysis demonstrated that the present *N*-demethylation is a clean reaction similar to the native enzyme system although the oxidation efficiency is rather less efficient than native one. We plotted the initial rates of *N*-demethylation catalyzed by Cyt-*c* bound to five different phosphate lipid bilayer membranes (**1a, 1b, 1c, 1e,** and **1d**) against their gel-to-liquid-crystal phase-transition temperatures ($T_c$ = 58, 48, 36, 30, and 18 °C, respectively).[28] As evident in Figure 9, an interesting feature is that the Cyt-*c* bound to the membranes in the liquid-crystalline

(27) Scott. R. A., Mauk, A. G., Eds. *Cytochrome c-A multidisciplinary approach*; University Science Book: Sausalito, CA, 1996.

(28) The phase-transition temperature of the lipid bilayer membranes was determined by differential scanning calorimeter (DSC). Although Figure 9 displayed the plot of the reaction rate at 38 °C, similar dependence was obtained at the reaction temperature of 30 °C.

state more effectively catalyze the reaction rather than the Cyt-*c* bound to the gel state membrane. No $T_c$ dependence was observed in the case of ammonium-lipid membranes. Thus, the membrane fluidity directly affects the intrinsic reactivity of the membrane-bound Cyt-*c*, in addition to the simple surface charge.

The structural study demonstrates that for the Cyt-*c* bearing the high spin-state of heme (**1a**-bound Cyt-*c*), the anisotropic lipid-binding causes the complete dissociation of the axial Met 80. The vacant axial site of the heme center is readily accessible to react with $H_2O_2$. This is clearly reflected by the enhanced affinity for $H_2O_2$ . On the other hand, the Cyt-*c* bearing the heme in a high-spin/low-spin equilibrium state shows different kinetic features. We conducted a kinetic study of **1d**-bound Cyt-*c* as a typical example. The affinity for $H_2O_2$ was 2.5-fold lower than that of **1a**-bound Cyt-*c*, whereas the catalytic efficiency was 10-fold greater. The increased $k_{cat}$ may have been due to the rapid exchange between the coordinated and uncoordinated Met 80. Dynamic swing of Met 80 in the axial site can facilitate the generation of the active species of heme that has reacted with $H_2O_2$. Such an increase in the dynamics of the active center is reflected in the observed accelerated heme degradation and autooxidation of the **1d**-bound Cyt-*c*.

We previously reported membrane-facilitated electron transfer and aniline hydroxylase activity of myoglobin.[29] These functions were ascribed to the unique capability of the lipid bilayer membrane to two-dimensionally organize plural functional molecules. The results of the present study established that specific binding of a lipid bilayer membrane alter the intrinsic activity of a native protein. Very recently, Sekimizu and coworkers reported that the activity of Dna A, an initiation protein of DNA replication, can be switched on by synthetic phosphate lipid membranes.[30] Based on these findings, we conclude that lipid bilayer membranes can operate as an active effector on protein molecules through both noncovalent and anisotropic interactions, as well as controlling the assembly of functional groups. Such interactions are potentially useful for protein-based bioengineering.

## Experimental Section

**Materials.** Horse heart cytochrome-c (Cyt-*c*, type IV) was purchased from Sigma Chemical Co. and purified by passing through a Sephadex G-25 column. The synthetic lipids were prepared according to the method reported previously by us[6,18a,31] and characterized by NMR, IR and elemental analysis. **1a**: Anal. Calcd for $C_{44}H_{84}NO_{13}P$: C, 64.38; H, 9.86; N, 1.63. Found: C, 64.19; H, 9.73; N, 1.67. **1c**: Anal. Calcd for $C_{38}H_{68}NO_{10}P$: C, 61.84; H, 9.17; N, 1.92. Found: C, 62.04; H, 9.17; N, 1.92. **1d**: Anal. Calcd for $C_{42}H_{75}NO_{12}P$: C, 61.81; H, 9.16; N, 1.72. Found: C, 61.97; H, 9.22; N, 1.78. **1e**: Anal. Calcd for $C_{43}H_{84}NO_9P$: C, 65.35; H, 10.74; N, 1.77. Found: C, 65.61; H, 10.76; N, 1.78. The synthesis of lipids **1b, 2a** and **2b** was reported previously.[18a,31] Other chemicals were commercially available.

**Assay Procedure for *N*-Demethylase Activity.** The *N*-demethylase activity of Cyt-*c* was assayed by measuring the amount of the produced formaldehyde using a modified Nash method.[21] Powdery lipids were suspended in 25 mM phosphate buffer (pH = 7.0) and sonicated at the appropriate temperatures (i.e., 5−10 °C higher than the corresponding $T_c$) for 3−10 min. In the case of the phosphate lipids, equimolar amount of NaOH was added before sonication. After the solution was incubated at room temperature overnight,[32] Cyt-*c* and NNDA was then added to the solution. The mixture was incubated for several minutes in a water bath equipped with a thermostatic controller (30 or 38 °C). The reaction was initiated by the addition of $H_2O_2$ and terminated by the addition of 30% trichloroacetic acid (TCA). After centrifugation of the reaction mixture at 15000 rpm for 20 min, 1 mL of the supernatant was mixed with Nash reagent (11.3 g of ammonium acetate, 150 uL of 2,4-pentanedione and 225 uL of acetic acid in 25 mL of $H_2O$) and the solution was incubated at 40 °C for 1 h. The absorbance of the resulting conjugate (3,5-diacetyl-1,4-dihydrolutidine) was monitored at 412 nm ($\epsilon_{412nm}$ = 7950 $M^{-1}$ $cm^{-1}$) on a Shimadzu UV2200 UV−visible spectrophotometer.

**Product Determination in N-Demethylation Reaction**. From the reaction mixture (20 mL scale), a 3 mL sample was taken out at 0, 2, 4, 6, 8, 10, 12 min and mixed with 0.9 mL of TCA. After centrifugation, the supernatant was applied to HPLC: column; a reversed-phase TOSOH, internal standard; *N*-ethylaniline,[22] eluent; acetonitrile/$H_2O$ (1/1, v/v)) at a flow rate of 1.0 mL/min. The amount of the unreacted $H_2O_2$ was determined as follows:[33] To the supernatant (1 mL), 0.2 mL of ferroammonium sulfate (10 mM, freshly prepared) and 80 $\mu$L of 2.5 M of KSCN were added. The solution was incubated for 10 min at 25 °C, and the absorbance at 480 nm was monitored.

**Binding Assay of Cyt-*c* to Lipid Bilayer Membranes.**[6] The solution containing Cyt-*c* and lipid membranes was ultrafiltered using a MOLCUT II system (UPF1 THK24, cut of molecular weight 100000; Millipore). The concentration of unbound Cyt-*c* was determined by the absorbance of the filtrate (408 nm).

**EPR Measurement and Simulation.**[18a,b] EPR measurements at 4 or 20 K, and the simulation for the orientation of the heme plane of Cyt-*c* against the film surface was conducted according to the reported method by us.

**CD Measurement.** CD spectra were obtained using a JASCO J-720 spectropolarimeter (sensitivity, 10 mdeg; resolution, 0.2 nm; bandwidth, 2.0 nm; response, 0.5 s; speed; 200 nm/min) at 25 °C.

**Acknowledgment.** The authors thank Mrs. Atsushi Baba and Takeshi Kawakami for the preparation of the synthetic lipids. We are also grateful to Mr. Hideki Horiuchi for his skillful preparation of the specially designed quartz plate for EPR measurements. This research is partially supported by the Foundation Advanced Technology Institute and Nissan Science Foundation.

JA9711775

(29) (a) Hamachi, I.; Fujita, A.; Kunitake, T. *J. Inorg. Biochem.***1993**, 51, 327. (b) Hamachi, I.; Fujita, A.; Kunitake, T. *Chem. Lett.* **1995**, 657.

(30) (a) Sekimizu, K. *Chem. Phys. Lipids.* **1994**, *73*, 223. (b) Mizushima, T.; Ishikawa, Y.; Obana, E.; Hasa, M.; Kubota, T.; Katayama, T.; Kunitake, T.; Sekimizu, K. *J. Biol. Chem.* **1996**, *271*, 3633.

(31) Nakashima, N.; Asakuma, S.; Kunitake, T. *J. Am. Chem. Soc.* **1985**, *107*, 509.

(32) The morphology of all of the lipid bilayer membranes was a mixture of tube, disk, and stringlike structures.

(33) Hildebrandt, A. G.; Roots, I.; Tjoe, M.; Heinemeyer, G. *Methods Enzymol.* **1978**, *52*, 342.